From geology to production: a completion optimization case study from Cleveland Sand, Oklahoma

Vivek Swami[1*], Graham Spence[1], Theophile Gentilhomme[1], Bob Bachman[1], Mark Letizia[1] and Casey Lipp[2] demonstrate that optimized stage spacing will result in the development of a larger SRV and higher production.

Introduction

Oil companies seldom acquire the necessary data to help them understand subsurface heterogeneity when they design multi-stage completions for lateral wells. In particular, well logs are rarely run in the lateral section. In the absence of such subsurface information, operators generally adhere to 'geometric' completion designs or equally spaced stages in the lateral section. While this approach seems reasonable and follows industry norms, it may not be very effective for heterogeneous rock (Far et al., 2015; Ashton et al., 2013; Ganguly and Cipolla, 2012). The geometric completion design may result in a limited stimulated reservoir volume (SRV) and lower well production than could be achieved with an optimized design based on subsurface information.

Geoscientists, completion engineers and reservoir engineers focus on different aspects of the complex problem of fracture spacing in a horizontal well. In the comprehensive study presented in this article, the authors have developed an integrated reservoir model combining reservoir characterization, petrophysical, geophysical, drilling and completion data. A fully coupled reservoir/geomechanical simulation model was built to capture the variation in rock properties in the lateral section, and to assess the impact of this variation on the simulation of injection and production processes. This single model was used to simulate both the injection and production times for the well.

This study is based on original work that was performed on horizontal wells in the Cleveland Sandstone Formation. Located in the Anadarko basin, Oklahoma, the Cleveland Sandstone formation is 100-300 ft thick and composed of low-permeability sands (ranging from 0.001 to 1.1 mD) deposited within a succession of highstand deltaic and lowstand incised valley-fill deposits. The reader is referred to our previous publication (Oliver et al., 2015) for more details. The authors describe the technique of using automated, quantitative mineralogy (RoqScan) to analyse readily available drill cuttings and derive rock property and elastic pseudo-logs based on bulk mineralogy and pore aspect ratio. Results can be used to customize completion designs to take into account reservoir heterogeneity along the lateral section. This is done in the absence of well logs in the lateral section. It was observed that the optimized completion rendered better frac initiation, lower stress shadow effects, better SRV growth, and higher proppant placement. Production was increased by 15% compared to what an analogous well with a geometric completion design would achieve.

We expand on the findings of that work to utilize the estimated elastic rock properties in a proprietary coupled reservoir-geomechanical simulator known as GeoSim. The geometry of the individual cluster fractures can then be computed during pumping in a realistic setting. Clean-up and long-term production is calculated within the same model. This allows investigation of different treatment stage designs within the lateral section of the well. GeoSim is a modular software system combining a 3D three-phase thermal reservoir simulator with a general 3D finite-element stress-strain simulator. The reader is referred to Settari and Walters, 2009 for a more holistic description of GeoSim. Simulations were history-matched to one of the wells from the previous study using the available treatment/production data. The study supports the idea that optimized stage spacing will result in the development of a larger SRV and higher production.

Workflow

The entire workflow for this study is summarized in the following steps:

1. Optimize perforation and stage placement
   - Acquire and analyse cuttings in the vertical and horizontal section using RoqScan
   - Calibrate rock physics module using acquired logs and cuttings
   - Generate synthetic logs in the horizontal section for rock mechanical properties
   - Place perforations and stages in the horizontal section to homogenize the stages
2. Generate 3D geological model
   - Acquire 3D seismic data and generate cubes for rock mechanical properties
   - Calibrate the seismic data with wells logs in the vertical section and RoqScan-generated logs in the horizontal section

[1] CGG | [2] Peregrine Petroleum
[*] Corresponding author, E-mail: vivek.swami@cgg.com

3. Production/mini-frac analysis
   - Analyse mini-frac and production data to extract SRV/ hydraulic fracture/reservoir properties
4. Simulation
   - Refine static reservoir grid with seismic constrained properties generated in step 2
   - History-match the model against treatment and production data
   - Run sensitivities on stage and perforation cluster spacing, injection rates, well spacing
   - Generate prediction for Estimated Ultimate Recovery (EUR)

Step 1 of the workflow was described in a previous publication (Oliver et al., 2015). The end result was that geometric fracture stage spacing was not used in the subject well. Stage spacing was determined by minimizing the mechanical property variation within a stage. Steps 2 through 4 are described in the following sections.

3D geological model

A fine-scale 3D geological model is created based on the RoqScan facies interpretation. Four different facies are defined based on the Young's Modulus (YM) and Poisson's Ratio (PR) ranges. Conditioned by the well, a 3D facies property is generated using Sequential Indicator Simulation. YM, PR, density, porosity and permeability are generated by Sequential Gaussian Simulation using the distributions and correlations observed in the RoqScan data, for each facies in the 3D cube. Those properties are then transferred to the simulation grid using the nearest cell method so that the property contrasts are preserved. Figure 1 shows the complete process from cuttings analysis to a 3D seismic constrained model.

Overview of the study well and available engineering data

The study well has a lateral section of approximately 5000 ft. A total of 21 frac stages were pumped over a four-day period. Each stage had four or five perforation clusters making a total of 100 perforation clusters. On average, each stage pumped 4700 bbl/stage of fluid, totalling nearly 100,000 bbl of fluid. For each stage, the average maximum rate achieved was between 60 and 80 bpm and the maximum surface injection pressure was 8700 psi.

After the injection, the well was shut-in for four months before being put into production. It began by producing injected water and subsequently started producing oil, with a decreasing water cut. Production data was available for approximately one year. Figure 2 shows the observed data for injection and production phases.

Production transient analysis

It is beneficial to examine the existing data using analytical techniques to understand the data's character before any simulation exercise. In particular, the production data can give considerable insight into the fracture and SRV properties. History matching can be performed much faster when an initial l estimate is obtained for the hydraulic fracture and SRV properties.

Analytical modelling can provide estimates for hydraulic fracture and reservoir parameters if proper flow regime identification and analysis can be performed. Rate Transient Analysis (RTA) was performed on the production data. It was conducted using an evaluation technique described by Wattenbarger et al. (1998), Arevalo-Villagran and Wattenbarger (1998), Economides et al. (2000), Liang et al. (2011), Bachman et al. (2011) and Swami et al. (2017).

The bottom hole pressure (BHP) and liquid production rate data was analysed using the specialized plots based on first-order material balance time (tmb) which is equivalent to cumulative oil/oil production rate (q). Delta p (Δp) is the difference between initial pressure and BHP, (i.e. $P_i - P_{wf}$). Figure 3 shows the diagnostic plot of log Δp/q vs log t_{mb}. The ½ slope line denotes formation linear flow and deviation from ½ slope line denotes end of formation linear flow. Based on this plot, we see the linear flow regime holds until t_{mb}=~300 days which corresponds to t=~150 days.

Next, we plotted the linear Δp/q vs sqrt t_{mb} in in Figure 4. The slope of the line shown gives a rough estimate of $x_f\sqrt{k_{SRV}}$, where k_{SRV} is the average SRV permeability and x_f is the fracture length. This calculation gives $x_f\sqrt{k_{SRV}}$ = ~30 $md^{0.5}$-ft. Based on the time when linear flow ends, a first-order estimation of k_{SRV} is also possible. This analysis gives k_{SRV} = 0.98 mD and x_f = 30 ft.

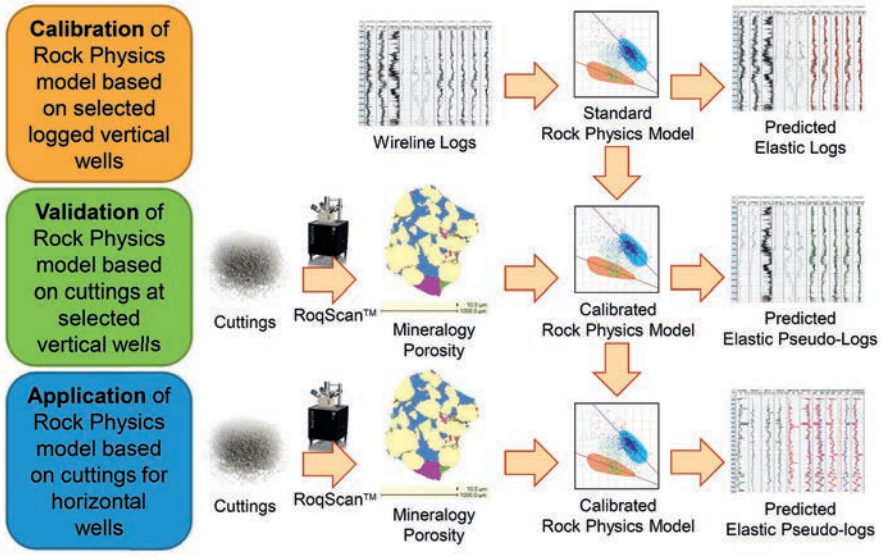

Figure 1 The calibration and prediction of elastic rock properties using quantitative automated mineralogical and pore space analysis of drill cuttings.

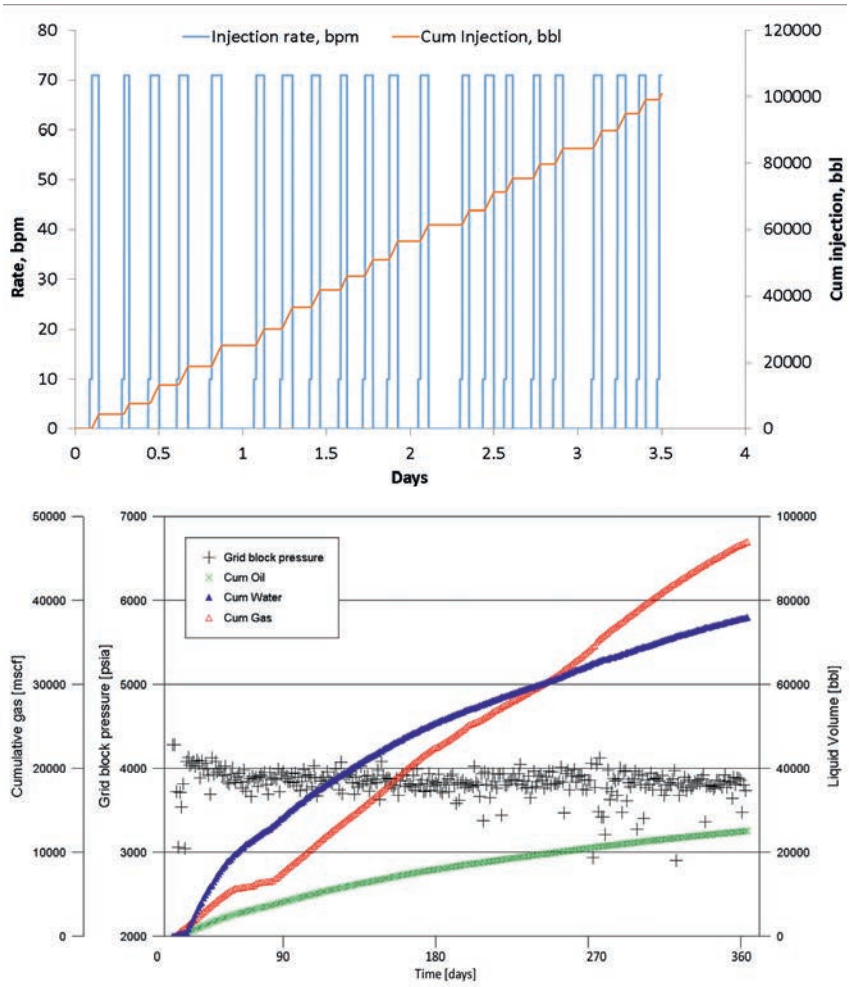

Figure 2 Plot of injection rate and cumulative volume vs time (simulation schedule) (top), plot of cumulative production volumes and bottom hole pressure (bottom).

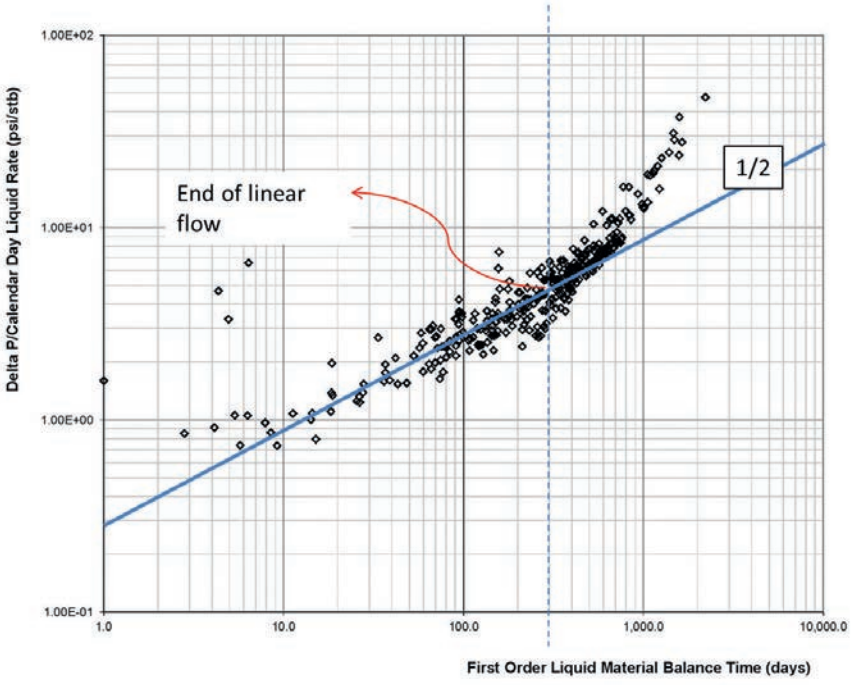

Figure 3 Log-log plot of Δp/q vs tmb showing linear flow.

Since the average base permeability is 40 µD or 0.04 mD, this corresponds to a residual permeability multiplier of 25.

It is noteworthy that this exercise gives a measure of the average residual permeability in the entire system. In reality, and in the simulation model proposed in this paper, each simulation cell has a different permeability enhancement and the residual permeability that is the function of the injection rate, peak pressure encountered during treatment, initial stress, YM and PR of that cell.

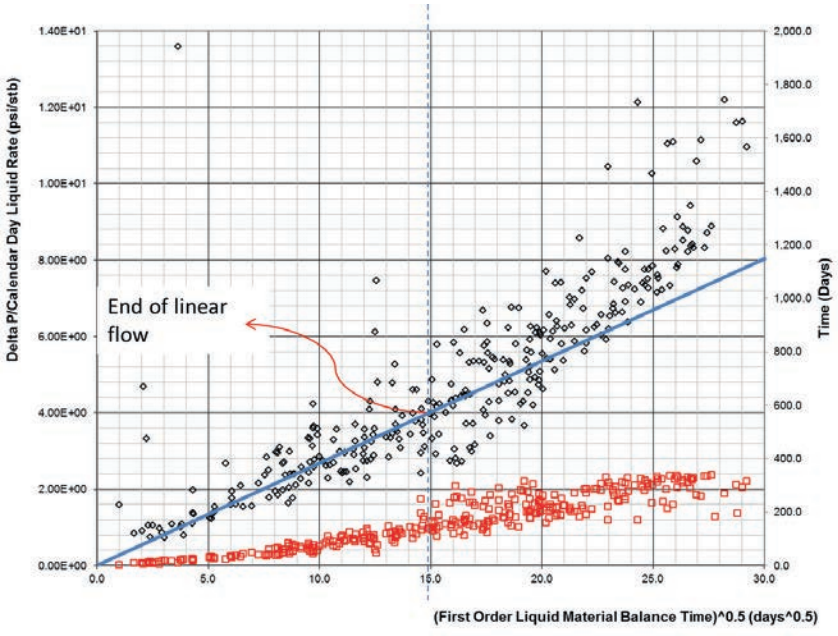

Figure 4 Δp/q and time vs √tmb plot. Black dots represent Δp/q and red dots represent time.

Simulation methodology

The study used the reservoir and geomechanical modelling techniques recently developed for shale reservoirs (Swami et al. 2017). One additional feature was incorporated into the modelling techniques for this work, i.e. the ability to capture the 3D variation in YM and PR.

Both the completion (injection) and historical production periods are matched using the same integrated model. This approach can be used to model a number of aspects of the treatment and production, which are rarely considered by other methods. As examples, during treatment, it can accommodate the stress shadow effect on subsequent stages and its effect during the production phase. Similarly, during the production phase it captures the effect of injected water on hydrocarbon production. The well model is capable of having an unlimited number of fractures and SRVs and handles the entire well treatment/clean-up/production history. Results show the importance of this integrated approach and give insight into many issues, such as the importance of cluster and stage selection on EUR.

Capturing permeability variation

The overall modelling system consists of a coupled 3D reservoir simulator and geomechanical module, together with a technique for modelling propagating fractures/SRV during stimulation. A further module handles the propped fractures during production. During stimulation, a single primary fracture will typically propagate from a perforation cluster, surrounded by a growing region of enhanced permeability consisting of a combination of the matrix permeability enhancement (microfracturing), reopening of the existing natural fracture system and the creation of new shear fractures. In the approach described in this article, the primary fracture propagating from each perforation cluster is modelled explicitly, while the SRV network is represented by a pseudo-continuum. Both processes are represented in the reservoir model by permeability enhancement as a function of effective stress. Open fractures or fractured media show a non-linear dependence of permeability on aperture which, in turn, is a function of closure stress or pressure. Additional practical applications have been described by Swami et al., (2017). The underlying theory can be found at Nassir et al. (2014), Goodarzi et al. (2012), Ji et al. (2009), Ji et al. (2004) and Settari et al. (2015).

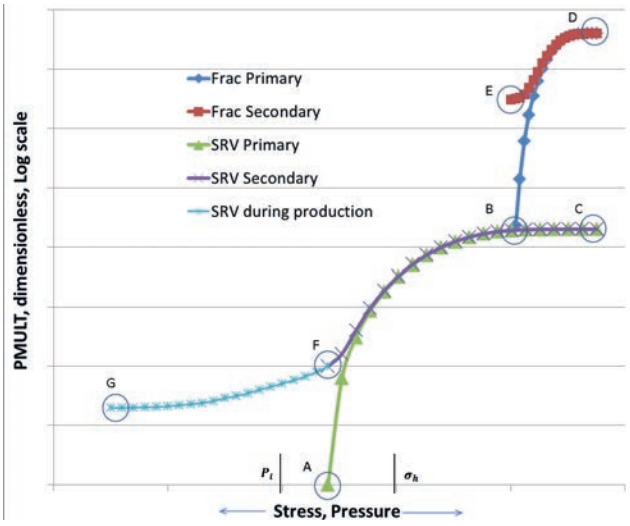

Figure 5 Permeability as a function of pressure/ stress during injection and production.

Figure 5 shows a generic plot for stress-dependent permeability functions in the matrix and hydraulic fractures. The green curve shows the primary permeability curve in the SRV when pressure rises, generally during the injection phase. The purple curve depicts the secondary or hysteresis curve in the SRV when the pressure falls, generally during a shut-in or the production phase. The light blue curve represents the permeability in the SRV during the production phase after the pressure has fallen to a point where the primary curve started. The dark-blue curve depicts the primary permeability in a hydraulic fracture when pressure rises, during the injection phase. The red curve depicts the secondary or hysteresis curve in the hydraulic fracture when pressure falls, generally during a shut-in or the production phase. Note that the SRV function is typically defined in a 3D region around the well, while the fracture functions only in grid planes in their propagation direction.

As injection starts in the reservoir, shear fractures develop first, followed by tensile fracture. At point A (somewhere between initial pressure, P_i and minimum horizontal stress, σ_h), a region of shear fracturing starts to develop, usually called the SRV. The system follows the SRV primary curve until pressure hits point B. At this point, tensile fractures start to develop and permeability follows the fracture primary curve until point D which corresponds to permeability at the maximum injection pressure. The SRV region where the hydraulic fracture did not develop continues to follow the SRV primary curve until point C which corresponds to permeability at the maximum injection pressure. At this point either the well is shut-in or starts producing, causing the pressure to fall. Consequently, permeability takes the path of the SRV secondary in the SRV and the frac secondary in the hydraulic fracture. In the hydraulic fracture, the permeability multiplier falls to point E which is governed by the proppant characteristic in addition to the stress in the system. In the SRV, the permeability multiplier follows the SRV secondary curve until point G via point F.

Capturing variation in Young's Modulus and Poisson's Ratio

To capture the variation in YM and PR across the reservoir model, a separate permeability function is constructed which is dependent upon grid block YM and PR values and the initial permeability. For efficiency, model cells are classified into 32 rock types with certain bounds for YM and PR. YM and PR values are upscaled to the grid level and assigned a rock type. There is an analogous porosity function dependent on YM and PR and the initial porosity in that cell. As an example, rock type 27 has 0.24 and 0.26 as the bounds for PR and 3.5 x 10^6 and 4.0 x 10^6 psi as the bounds for YM. This specific cell is shown with a solid black in Figure 6. There were 16,668 blocks satisfying this criterion (total grid blocks in this model are 558,624). The average PR of all such blocks is then 0.244 and average YM is 3.705 x 10^6 psi.

Relative permeability

In our experience, Corey's exponent models for relative permeability are appropriate for tight gas reservoirs such as the Cleveland Sand. Based on the history match, Corey's exponents for the relative permeability functions were n_{ow}=2.6 (oil curve for water-oil displacement), n_w=2.4 (water curve), n_{og}=1.5 (oil curve for gas-oil displacement) and n_g=1.7 for gas.

Simulation model

The simulation model uses a flexible grid size definition to increase resolution in the vicinity of the well and perforations and reduce the resolution away from the well. The grid was refined along the Y direction (i.e. direction of the well) to 1 ft cells at the perforation locations. Grid cells were gradually coarsened away from the perforation locations. Consequently, the grid dimensions were 33 x 1058 x 16 covering 1140 x 5550 x 1310 ft in the X-Y-Z directions with the total number of grid blocks in the model being 558,624. The grid extended 570 ft on either side of the subject well in the X direction and 500 ft above and below in the Z direction to accommodate all fracture growth and other geomechanical effects (stress changes).

The pay zone is around 40 ft thick bounded by approximately 100 ft of Mid Cleveland on the top and 100 ft of Lower Cleveland at the bottom. Approx. 500 ft of overburden and 500 ft of underburden were kept in the model to accommodate all fracture growth and other geomechanical effects (stress changes). The geologic model was flattened to have the pay zone top at 9242 ft. Figure 7 shows the elevation view for the reservoir horizontal permeability profile at time=0. It also shows the relative position of the well in the reservoir.

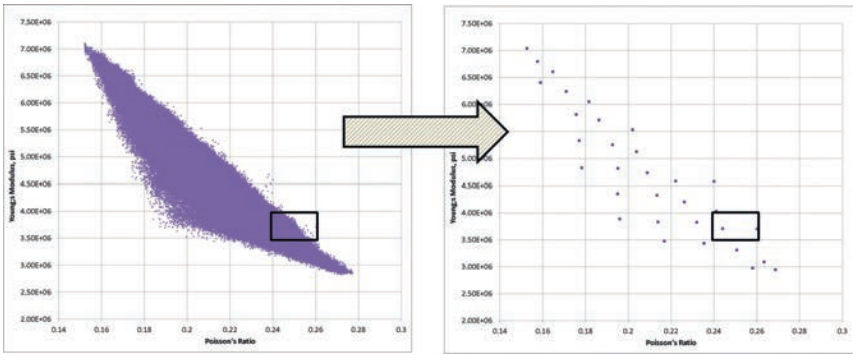

Figure 6 Classification of model cells into 32 rock types.

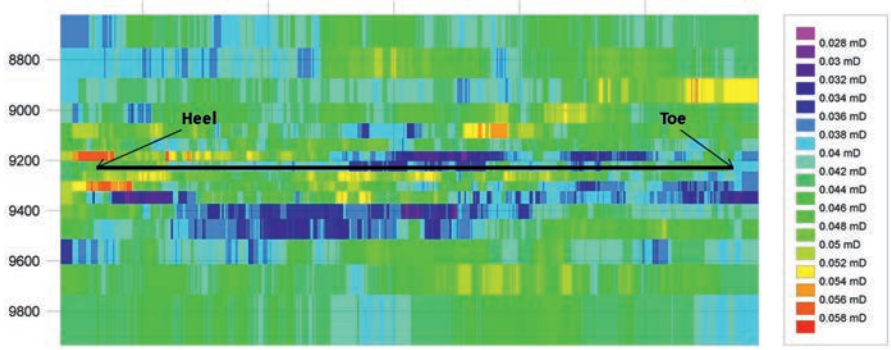

Figure 7 Elevation view for reservoir permeability.

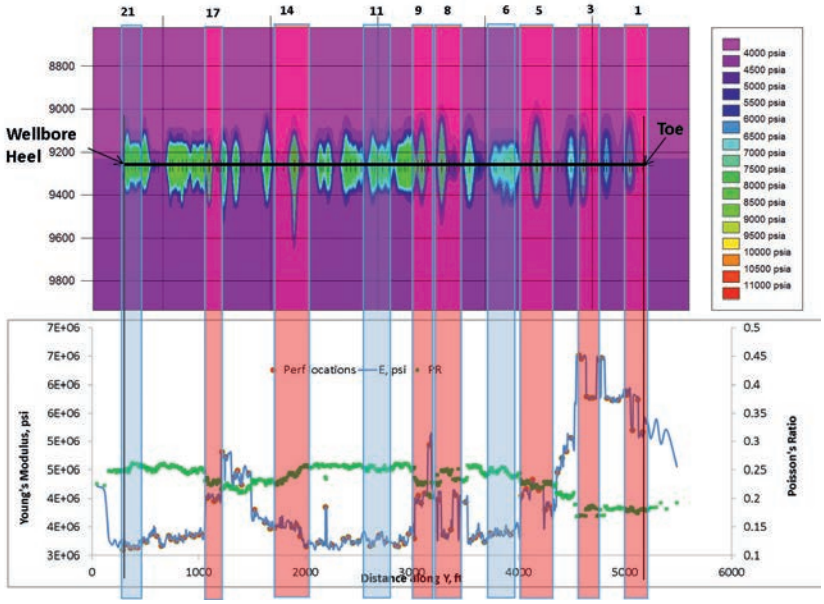

Figure 8 Reservoir pressure after injection of all 21 stages in cross section along the well (top) and Poisson's ratio, Young's modulus and perforation locations (bottom).

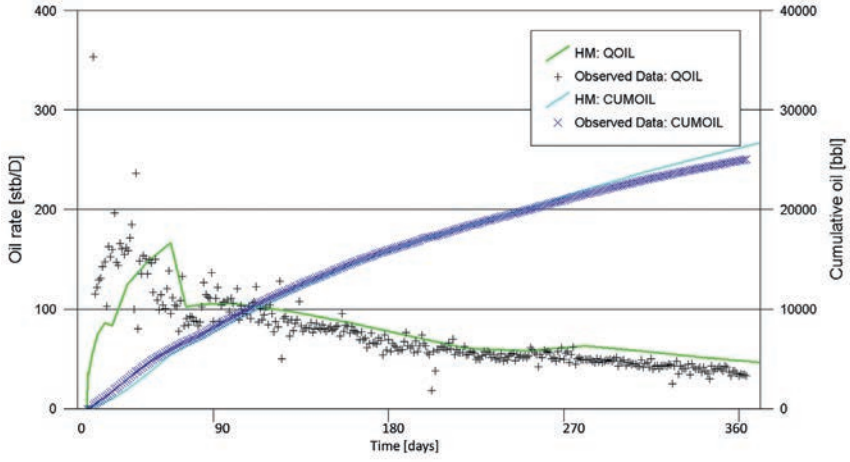

Figure 9 Observed vs history-matched oil production rate and cumulative oil production. Solid lines show the simulated oil rate (green) and cumulative oil (cyan) and points show the observed oil rate (black cross) and cumulative oil (blue cross).

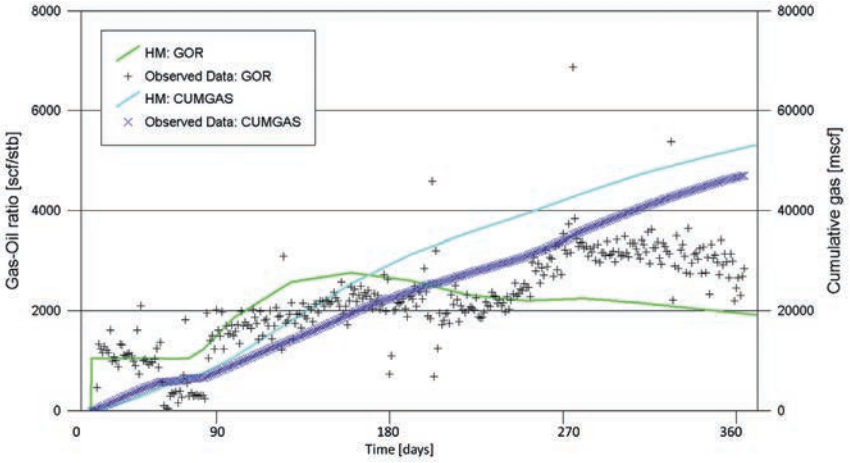

Figure 10 Observed vs HM Gas-Oil ratio and cumulative gas production. Solid lines show the simulated GOR (green) and cumulative gas (cyan) and points show the observed GOR (black cross) and cumulative gas (blue cross).

Simulation of injection phase

For treatment injection, it was assumed that a fracture could initiate from each perforation cluster and fractures were allowed to grow perpendicular to the well. As described earlier, a sufficiently large overburden and underburden were kept in the model to accommodate fracture growth during the treatment phase. Note that the well is aligned parallel to minimum horizontal stress to ensure hydraulic fractures grow transverse to the well. A fracture gradient of 0.71 psi/ft was assumed. This resulted in a minimum horizontal stress (S_{hmin}) of 6,575 psi for the subject well.

Figure 8 shows the reservoir pressure in the plan view of the model, after pumping all the stages. The model accounted for all 21 stages and the individual clusters. Each stage was individually modelled as per the hydraulic fracturing report with appropriate shut-ins between stages. The observed injection volumes and treatment pressures were honoured during this phase.

Figure 8 also shows the profiles of Young's modulus (YM), Poisson's ratio (PR) and perforation placement along the well. In general, the higher the Young's modulus, the higher the rock brittleness and the easier it is to initiate and propagate hydraulic fractures. Poisson's ratio variation does not affect the hydraulic fracture behaviour very significantly. Furthermore, higher YM implies thinner (lower width) and hence longer fractures. The aim of stage selection is to have high homogeneity with respect to YM and PR within a stage. But simultaneously, the aim is also to stimulate the entire well. Optimization of the stages and cluster spacing is required. As examples, stages 6, 11 and 21 are fairly homogeneous whereas stages 1, 5 and 14 are not. The homogeneous stages are shown in blue whereas the heterogeneous ones are shown in red. All the perforations within a homogenous stage (such as 6, 11 and 21) took fairly equal volumes resulting in fairly uniform hydraulic fractures and efficient stimulation. On the other hand, the heterogeneous stages (e.g. 1, 5 and 21) cause the perforation with the highest Young's modulus to take most of the fluid resulting in a less efficient stimulation.

Simulation of production phase and history matching

During injection it was assumed that all perforation clusters were open to injection and resulted in fracture propagation. During clean-up and production it was assumed that all propped fractures were connected to the wellbore. In our experience, the contributing propped fracture length during production is typically 40-60% of pumped treatment length. For this study the propped lengths were assumed to be 60% of the individual treatment lengths. The dynamic hydraulic fracture permeability multipliers were removed just before the well was opened for production and replaced with static propped fractures at each perforation set. Static fracture modelling is described by Miranda et al., (2010). Input length and fracture conductivity for the static fractures were important inputs for the pressure match, as was the residual SRV permeability multiplier for the reservoir matrix.

The production phase of the model was run with specified historical liquid rates and the water cut, gas-oil ratio (GOR) and bottom hole pressure (BHP) responses were calculated and matched. The average of external gauge data was used as the observed data. Figures 9, 10, and 11 show the comparison of the history-matched simulation case vs observed data for oil, gas and water production.

Figure 12 shows the history-matched case vs observed data for BHP. It is important to note that we were able to match the early water production, which is sensitive to the hysteresis parameters and relative permeability data. Symbols depict observed data and solid lines represent simulation results.

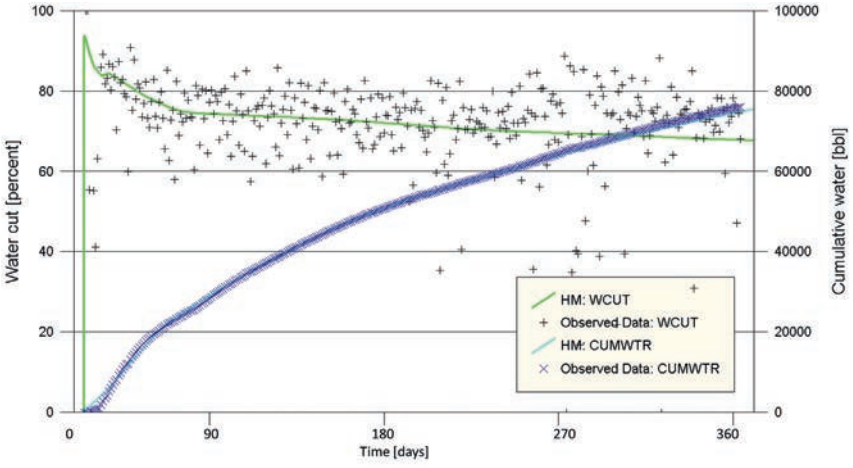

Figure 11 Observed vs HM water cut and cumulative water production. Solid lines show the simulated water cut (green) and cumulative water (cyan) and points show the observed water cut (black cross) and cumulative water (blue cross).

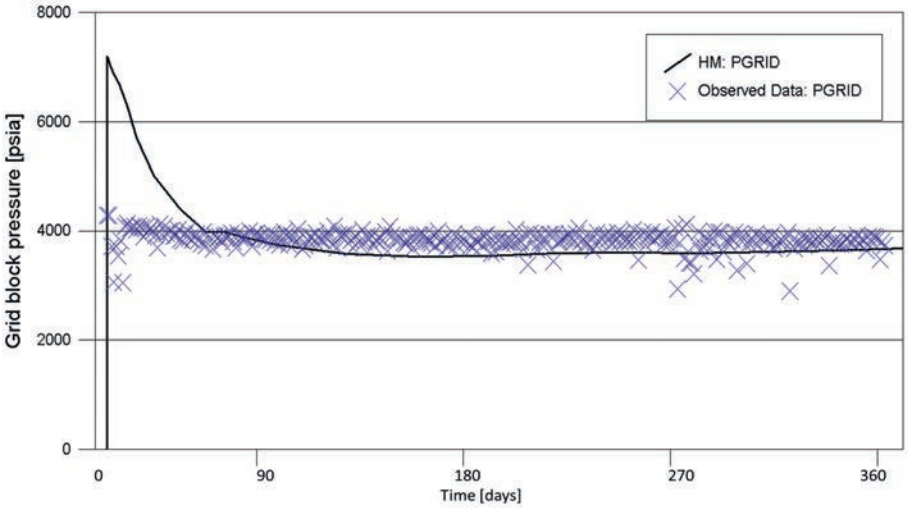

Figure 12 Observed vs HM BHP during production for the HM case. Solid lines show the simulated pressure (black) and points show the observed BHP (blue cross).

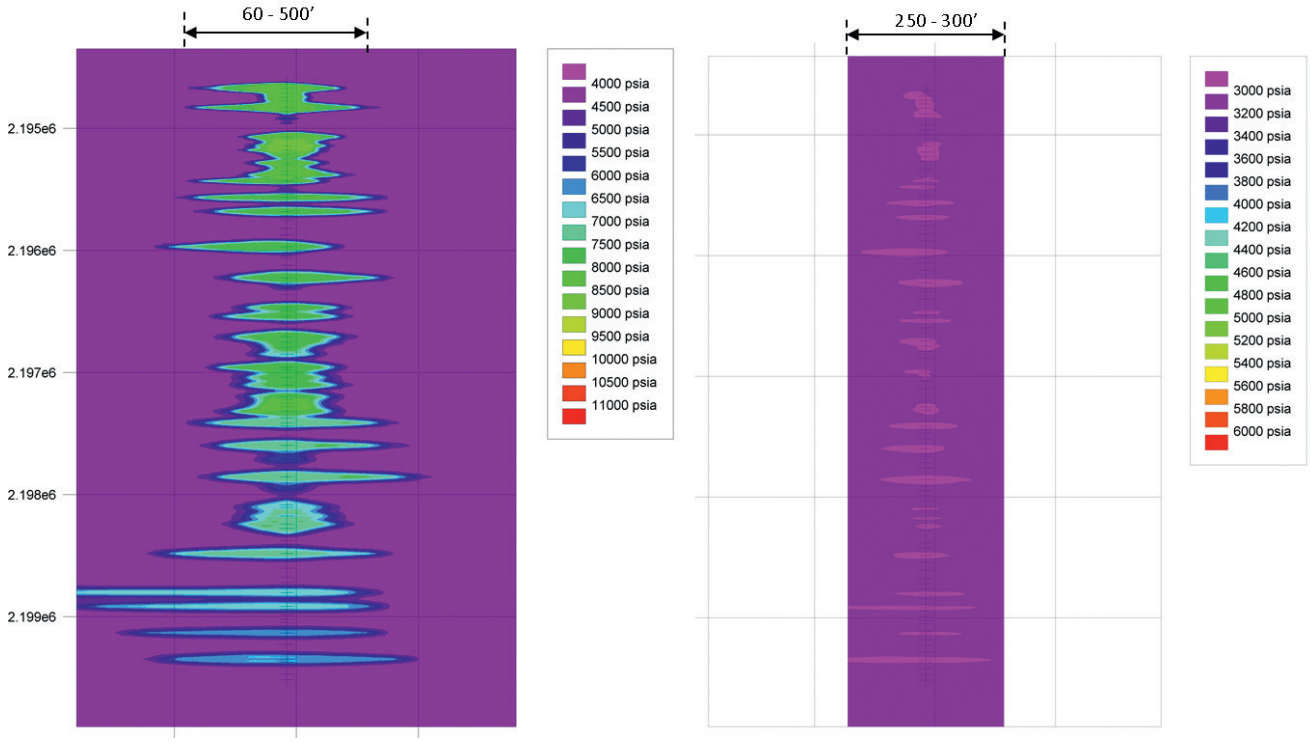

Figure 13 Pressure plot after injection (left) and 1000 days of production (right) for the history match case.

Discussion on history match case

Given the complexity of the problem, an acceptable history match was achieved. Overall, the chosen completion design in terms of cluster spacing, clusters/stage, stage spacing and stage rates adequately covers the wellbore length given the constraints (see Figure 13). The left side shows the pressure plot (in Layer 9) for the reservoir section at the end of injection, and the right side shows the depletion of the SRV after 50 years of production. After injection, the stimulated length was around 60 to 500 ft. depending on which hydraulic fracture was analysed. On the other hand, the average drainage length was around 250 to 300 ft. This translates to approximately 125 to 150 ft on either side of the well. This in turn implies that any well spacing of more than 150 ft. needs to be more rigorously evaluated.

Optimized vs geometric completion

The next step in the puzzle is to check the efficacy of optimized completion vs a geometric completion. To achieve that, a case was built with geometric (non-optimized) completion. All the stages and perforations were now equally spaced. While the number of perforations was kept the same as in the optimized case, i.e. 100, the number of stages was now 20. Each stage has five perforation clusters. Total treatment volume and peak injection rates were the same as in the geometric case. Table 1 shows a comparison of the two cases.

Figure 14 shows the plan view of pressure, at the end of the injection period, for the two approaches. The top part of the figure shows the geometric case, the bottom part shows the optimized case. In the geometric case, typically one perforation cluster within a stage takes all the injection fluid into one dominant fracture within a stage owing to the heterogeneity of YM and PR across the stage. On the other hand, in the optimized case, the YM, PR,

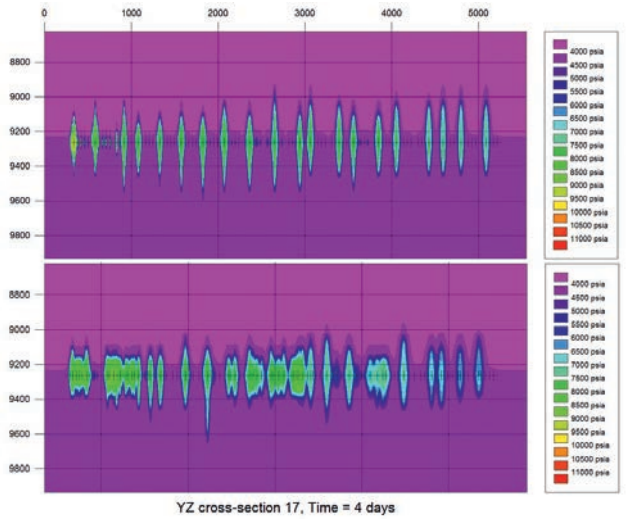

Figure 14 Pressure plot after injection for geometric (top) and optimized (bottom) stage spacing.

fracture initiation and therefore fluid distribution is much more uniform across the perforation clusters. Consequently, the optimized case yields a bigger SRV compared to the geometric case.

The stimulated zone strongly affects the production behaviour. Figure 15 shows the comparison of predicted oil, gas and water production for the optimized and geometric cases over a period of 50 years. It was found that an optimized completion renders over 15% more production than a geometric completion for the same well properties.

Summary and conclusions

This study shows the benefit of an optimized completion design with variable stage spacing. Completion optimization

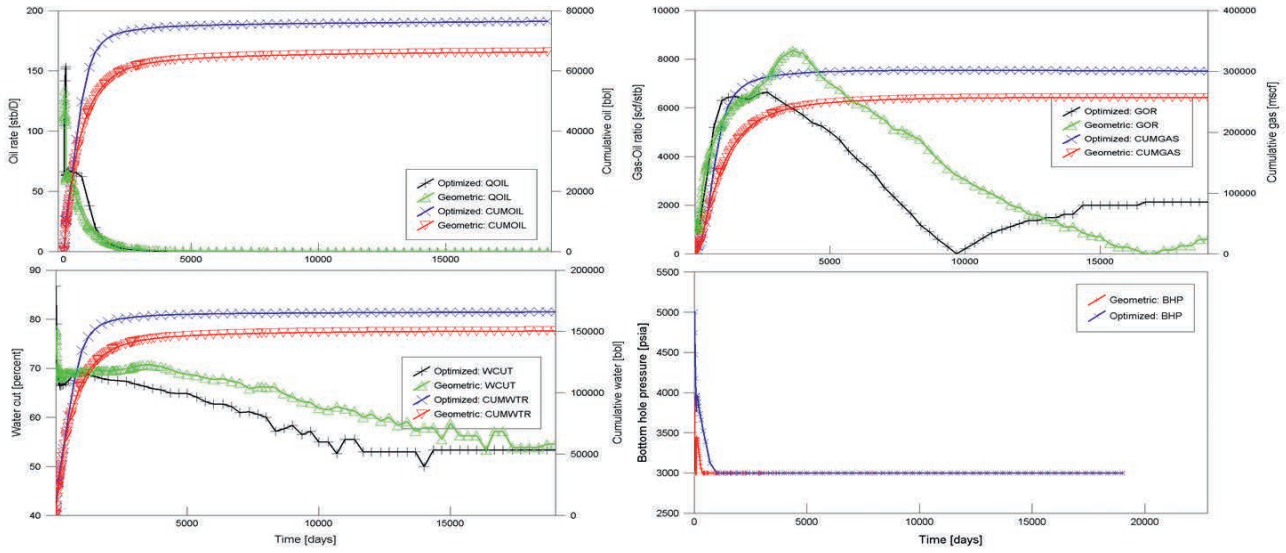

Figure 15 Pressure plot after injection for geometric (top) and optimized (bottom).

Parameter	Optimized completion	Geometrical completion
Stage spacing, ft	52-108	80
Perforation spacing, ft	16-60	42
Total stages	21	20
Perforations	4/5 per stage, total 100	5 per stage, total 100
Total fluid injected, in ,000 bbl	116	116

Table 1 Summary of fracture and SRV from three injection simulation scenarios.

was carried out using elastic rock property data derived from automated quantitative mineralogy and pore space analysis of drill cuttings with CGG's proprietary RoqScan technology. A coupled reservoir-geomechanical simulator modelling all the essential features of the well was able to history-match well behaviour. A comparative geometric stage spacing run was then made to quantify the loss in production from a sub-completion strategy.

The following conclusions can be drawn from this exercise:

1. Coupled reservoir/geomechanics simulation successfully captures the effect of changes in geomechanical parameters (Young's modulus, Poisson's ratio, effective stresses) compared to uncoupled simulation methodologies.
2. Hydraulic fractures within a stage were found not to be equal. It was observed from this simulation that heterogeneity within a stage causes uneven distribution of frac fluid across the perforation clusters which results in a reduced SRV.
3. The entire hydraulic fracture and SRV do not contribute to production. On average, 60% of treatment lengths were found to be contributing to the production.
4. Analytical models for production analysis provided valuable insights into the hydraulic fracture properties. They gave a good first-hand estimate of fracture half-length and SRV residual permeability.
5. Simulations indicate that completion optimization (in terms of stage spacing and location) resulted in a 15% increase in production compared to the geometric case for this specific test well.

Acknowledgements

The authors would like to thank CGG and Peregrine Petroleum for allowing the release of their information for this publication and providing the necessary support to the authors to work on this paper.

References

Arevalo-Villagran, J.A. and Wattenbarger, R.A. [1998]. *Long Term Linear Flow in Gas Wells.* Personal communication with Bob Bachman.

Ashton, T., Ly, C.V., Spence, G. and Oliver, G. [2013]. Portable Technology Puts Real-time Automated Minerology on the Well Site. *SPE URC*, Extended Abstract.

Bachman, R.C., Sen, V., Khalmanova, D., M'Angha, V.O., Settari, A. [2011]. Examining the Effects of Stress Dependent Reservoir Permeability on Stimulated Horizontal Montney Gas Wells. *CSUG/SPE Conference*, SPE 149331.

Economides, M.J., Nolte K.G. [2000]. *Reservoir Stimulation*. 3rd ed., Chapter 12: Post Treatment Evaluation and Fractured Well Performance, John Wiley & Sons.

Far, M.E., Buller, D., Quirein, J., Gu, M. and Gokaraju, D. [2015]. A new Integrated Data Analysis Algorithm and Workflow for Optimizing Horizontal Well Completion in Unconventional Reservoirs. *SPWLA 56th Annual Logging Symposium*, Expanded Abstracts

Ganguly, U. and Cipolla, C. [2012]. Multidomain Data and Modeling Unlock Unconventional Reservoir Challenges. *JPT Technology Update*, 32-37.

Goodarzi, S., Settari, A. and Keith, D. [2012]. Geomechanical modeling for CO2 storage in Nisku aquifer in Wabamun Lake area in Canada.

International Journal of Greenhouse Gas Control, **10** (9), 113-122, doi: 10.1016/j.ijggc.2012.05.020.

Ji, L., Settari, A. and Sullivan, R.B. [2009]. A Novel Hydraulic Fracturing Model Fully Coupled with Geomechanics and Reservoir Simulator. *SPE Journal*, **14** (3), 423-430.

Ji, L., Settari, A., Sullivan, R.B. and Orr, D. [2004]. Methods For Modeling Dynamic Fractures In Coupled Reservoir And Geomechanics Simulation. *SPE Annual Tech. Conf. and Exhib.*, SPE 90874.

Liang, P., Mattar, L. and Moghadam, S. [2011]. Analyzing Variable/Rate Pressure Data in Transient Linear Flow in Unconventional Gas Reservoirs. *Canadian Unconventional Conference*, SPE 149472.

Miranda, C., Soliman, M.Y., Settari, A. and Krampol, R. [2010]. Linking Reservoir Simulators with Fracture Simulators. *SPE Eastern Regional Meeting*, Abstracts.

Nassir, M., Settari, A. and Wan, R. [2014]. Prediction of SRV and Optimization of Fracturing in Tight Gas and Shale Using a Fully Elasto-Plastic Coupled Geomechanical Model, 163814-PA. *SPE Journal Paper*.

Oliver, G., Spence, G., Davis, A., Stolyarov, S., Gadzhimirzaev, D., Ackley, B. and Lipp, C. [2016]. Advanced cuttings analysis provides improved completion design, efficiency and well production. *First Break*, **34** (2), 64-72.

Settari, A. and Walters, D.A. [2001]. Advances in Coupled Geomechanical and Reservoir Modeling With Applications to Reservoir Compaction. *SPE Journal*, **6** (3), 334-342.

Settari, A., Sullivan, R.B., Turk, G., Rother, R. and Skinner, T. [2015]. Comprehensive coupled modeling analysis of stimulations and post-frac productivity – methodology and case study of the Wyoming field. *Hydraulic Fracturing Journal*, **2** (3), 45-50.

Settari, A., Nassir, M. and Sen, V. [2015]. Coupled reservoir and geomechanical numerical modeling of water injection into dynamically fractured formation. *SIAM Conference on Mathematical & Computational Issues in the Geosciences*, presentation.

Swami, V., Settari, A., Sahai, R., Costello, D. and Mercer, A. [2017]. A Novel Approach to History Matching and Optimization of Shale Completions and EUR – A Case Study of Eagle Ford Well. *SPE Unconventional Resources conference*, SPE 185175, doi:10.2118/185075-MS.

Wattenbarger, R.A., El-Banbi, A.H., Villega, M.E. and Maggard, J.B. [1998]. Production Analysis of Linear Flow in Fractured Tight Gas Wells. *SPE Rocky Mountain Regional Low-Permeability Reservoirs Symposium and Exhibition*, SPE 39931.